

**Oscillations and waves in metal-ion-catalyzed  
bromate oscillating reactions in highly oxidized states**

Anatol M. Zhabotinsky, Frank Buchholtz, Anatol B. Kiyatkin, and Irving R. Epstein

*J. Phys. Chem.*, **1993**, 97 (29), 7578-7584 • DOI: 10.1021/j100131a030 • Publication Date (Web): 01 May 2002

Downloaded from <http://pubs.acs.org> on March 31, 2009

**More About This Article**

---

The permalink <http://dx.doi.org/10.1021/j100131a030> provides access to:

- Links to articles and content related to this article
- Copyright permission to reproduce figures and/or text from this article



## Oscillations and Waves in Metal-Ion-Catalyzed Bromate Oscillating Reactions in Highly Oxidized States

Anatol M. Zhabotinsky,<sup>\*,†,‡</sup> Frank Buchholtz,<sup>\*,†,§</sup> Anatol B. Kiyatkin,<sup>‡</sup> and Irving R. Epstein<sup>\*,†</sup>

Department of Chemistry, Brandeis University, Waltham, Massachusetts 02254,  
and National Scientific Center of Hematology, Moscow, Russia

Received: February 5, 1993; In Final Form: May 12, 1993

A mathematical model of the Belousov–Zhabotinsky (BZ) oscillating reaction is presented along with experimental data showing that the catalyst can remain almost completely oxidized during a significant part of the oscillatory cycle in the ferroin-catalyzed BZ reaction. The model semiquantitatively describes oscillations and wave propagation in both the cerium- and ferroin-catalyzed systems when the phase of catalyst oxidation occupies a significant part of the oscillatory cycle. Such modes are of special interest because they give rise to enhanced instability of the bulk oscillations, enlargement of the number of local wave sources, and decremental wave propagation. Reversibility of the catalyst oxidation by bromine dioxide radicals is crucial for the dynamics of the system under these conditions.

### Introduction

The Belousov–Zhabotinsky (BZ) reaction–diffusion system is widely used for the study of chemical waves.<sup>1,2</sup> In most cases, the length of the excited region immediately following the wave front is short in comparison with the wavelength. However, the relative length of the excited part of the wave increases with the ratio of the bromate concentration ( $A$ ) to that of malonic acid ( $B$ ). Increasing this ratio also leads to increase of the number of wave-emitting centers<sup>3,4</sup> and to the loss of stability of spatially uniform bulk oscillations.<sup>5,6</sup> These findings correlate with those in generic models of excitable extended systems, where the emergence of wave-producing centers in nonoscillatory media is greatly favored by an increase in the ratio of the duration of the excited state to that of the refractory state.<sup>7,8</sup>

The term decremental propagation is used in electrophysiology to denote propagation of pulses with decreasing amplitude over a limited distance. In parameter space, this mode separates stationary, self-sustained propagation from total nonpropagation. Smoes<sup>9</sup> observed a new mode of wave propagation in the ferroin-catalyzed BZ reaction with relatively high  $A/B$  ratio. The bulk of the system is in the oxidized (blue) state. Circular red wave fronts with an increased ferroin concentration emerge from point pacemakers and slowly propagate outward. At the rear of each wave an oxidized region soon appears. These reduction to oxidation wave backs propagate with higher velocity than the leading oxidation to reduction fronts. As a result, the former overtake the latter, and the waves disappear at a finite distance from the pacemaker. We believe that these observations constitute the first example of decremental propagation of chemical waves. Tyson and Fife<sup>10</sup> gave a qualitative description of this mode of wave propagation, but they suggested that in the experiment the apparent wave cancellation resulted from the low optical contrast and that stationary wave propagation may actually be established. However, it is known that decremental wave propagation is possible.

These considerations suggest that study of the space–time behavior of the BZ system with large  $A/B$  ratio should prove interesting. Unfortunately, the existing mathematical models of the BZ reaction fail to describe correctly the modes of oscillation and wave propagation that appear under these conditions. The speed and shape of chemical waves in the Ce-catalyzed BZ reaction–diffusion system were studied in experiments and in a mathematical model by Nagy-Ungvarai et al.<sup>11,12</sup> They found for the first time the correct shape of the ceric ion concentration wave profile in an Oregonator-type model with a relatively large ratio of bromate to malonic acid concentration, for which the oxidized part of the wave occupies a significant part of the cycle.<sup>12</sup> However, they failed to obtain the correct dependence of the wave velocity on the bromate concentration.<sup>11</sup>

The principal positive and negative feedbacks in the mechanism of the BZ reaction<sup>13,14</sup> were studied in refs 15–18. The detailed mechanistic study of the BZ reaction began with the paper by Field, Körös, and Noyes,<sup>19</sup> who presented the FKN scheme, a skeleton mechanism of the reaction. Field and Noyes<sup>20</sup> then proposed the Oregonator model, a simplification of the FKN mechanism, in which the most efficient yet restrictive feature was the replacement of the complex organic reaction network that produces the inhibitor  $Br^-$  by a simple stoichiometric relation between the rates of catalyst reduction and inhibitor production.

The original Oregonator model<sup>20</sup> failed to describe correctly the shape of the oscillations. Rovinsky and Zhabotinsky<sup>21</sup> showed that the reversibility of quasidelementary reactions of the catalyst species was primarily responsible for the waveform. Later the mechanistic description and mathematical modeling of the BZ reaction were improved with the inclusion of the reversibility of certain quasi-elementary steps, addition of new steps, and more precise estimation of the rate constants.<sup>1,22,23</sup>

Still, the improved mathematical models of the BZ reaction fail to describe correctly the shape of the oscillations when the major portion of the catalyst remains oxidized during a relatively large part of the oscillation cycle. The reason for this failure is the tendency of all the Oregonator-related models to treat  $[BrO_2^*]$  as a fast variable with respect to  $[HBrO_2]$ .

Here we present experimental data on the waveform in the ferroin-catalyzed BZ reaction with high  $h_0A/B$  ratio, where  $h_0$  is Hammett's acidity function,<sup>24</sup>  $A$  is the bromate concentration,

<sup>†</sup> Brandeis University.

<sup>‡</sup> National Scientific Center of Hematology.

<sup>§</sup> Present address: Institut für Physikalische Chemie, Universität Würzburg, Markusstrasse 9-11, 8700 Würzburg, Germany.

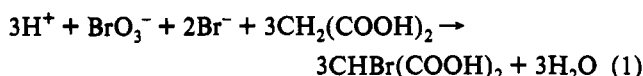
and  $B$  is the sum of concentrations of malonic and bromomalonic acid. In this case, the catalyst remains completely oxidized during a considerable part of the oscillatory cycle. We used bromomalonic acid produced by two different methods because a recent paper by Försterling et al.<sup>25</sup> showed that the method<sup>26</sup> widely used in studies of the chemical wave propagation gives a mixture with a low content of bromomalonic acid.

We present an improved mathematical model of the Oregonator type,<sup>1,20,21</sup> which accurately simulates the waveform in this concentration region for both the ferriin- and the cerium-catalyzed BZ reactions. The correct dependence of the trigger wave velocity on the bromate concentration is obtained for the cerium-catalyzed BZ system. The decremental mode of wave propagation is found, in accordance with the observations of Smoes.<sup>9</sup>

### Experimental Section

Sodium bromate, malonic acid (Aldrich), ferrous sulfate (Fisher), and 1,10-orthophenanthroline (Fluka) were of analytical grade.

We prepared dipotassium bromomalonate with the same <sup>13</sup>C NMR spectrum as described by Försterling et al.<sup>25</sup> Solutions containing bromomalonic acid were prepared by the following reaction in aqueous solution:<sup>26</sup>



The ferriin concentration was monitored as optical absorbance at 650 nm. Experiments were carried out at  $T = 25^\circ\text{C}$ . When a CSTR was used, the residence time was 35.6 min.

**Simulation of Wave Propagation.** Calculations were made for a one-dimensional reaction-diffusion system. The partial differential equations were transformed into a set of ordinary differential equations whose number is given by the number of spatial grid points times the number of variables. For the cerium-catalyzed system, 200 equidistant grid points were used, corresponding to a real length of 14 mm. For the ferriin-catalyzed system, 400 grid points covered a length of 18 mm. Higher spatial resolution and/or smaller time steps did not change the results. Zero-flux (Neumann) boundary conditions were used.

For the ferriin case, after the model was put into dimensionless form (see Appendix), the variable  $z$  corresponding to the relative concentration of ferriin was replaced by

$$a = \frac{1}{\epsilon + 1 - z}$$

where  $\epsilon = k_8/k_{-7}h_0C$  and  $C$  = total catalyst concentration. This procedure allows for 100-fold larger time steps when the backward Euler scheme<sup>27</sup> is used for numerical integration.

**Shape of Ferriin Oscillations in Highly Oxidized States.** As noted in the Introduction, the waveform in the BZ reaction is primarily determined by the ratio  $A/B$  (where  $A$  is the initial concentration of bromate and  $B$  is the sum of the initial concentrations of malonic and bromomalonic acids). More generally, the waveform is governed by the ratio  $W = h_0A/B$ .

Figure 1a shows the shape of the ferriin concentration oscillations in a CSTR when  $W = 6.6$ . The part ( $T_1$ ) of the cycle during which the ferriin concentration is practically zero exceeds 40% of the total oscillation period ( $T$ ).

Figure 1b shows the same shape of oscillations in a batch system with  $[\text{CH}_2(\text{COOH})_2]_0 = 0.012\text{ M}$  and  $[\text{CHBr}(\text{COOK})_2]_0 = 0.006\text{ M}$ . Analogous records were obtained with BrMA produced as in ref 26 when its nominal initial concentration was 0.03 M according to eq 1; this corresponds approximately to  $[\text{CH}_2(\text{COOH})_2]_0 = 0.012\text{ M}$  and  $[\text{CHBr}(\text{COOH})_2]_0 = 0.006\text{ M}$  according to data from ref 25. In the batch system, the amplitude of oscillations decreases and the  $T_1/T$  ratio increases owing to

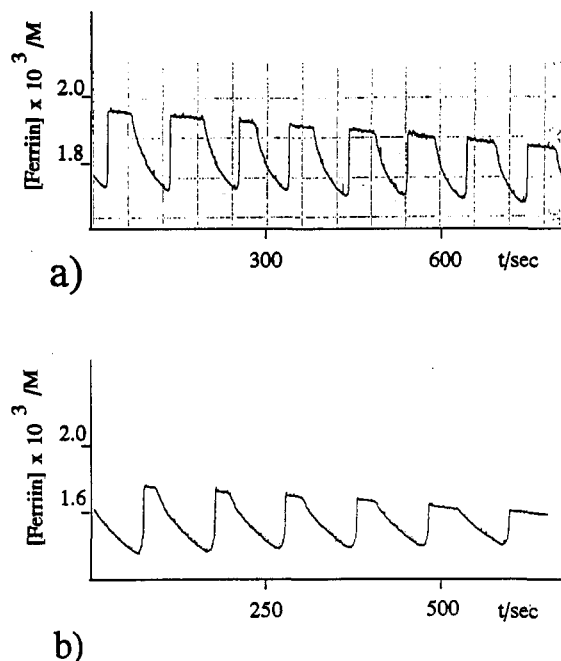


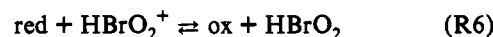
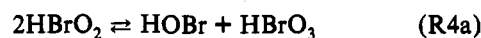
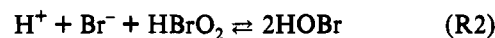
**Figure 1.** Ferriin concentration oscillations in systems with high values of  $W = h_0A/B$ . (a) Oscillations in a CSTR with residence time 35.6 min. Initial reagent concentrations (M):  $\text{NaBrO}_3$ , 0.25;  $\text{CH}_2(\text{COOH})_2$ , 0.01;  $\text{CHBr}(\text{COOH})_2$ , 0.002;  $\text{Fe}(\text{phen})_3$ , 0.002;  $\text{H}_2\text{SO}_4$ , 0.3. (b) Oscillations in a batch system. Initial reagent concentrations (M):  $\text{NaBrO}_3$ , 0.25;  $\text{CH}_2(\text{COOH})_2$ , 0.012;  $\text{CHBr}(\text{COOK})_2$ , 0.006;  $\text{Fe}(\text{phen})_3$ , 0.002;  $\text{H}_2\text{SO}_4$ , 0.3.

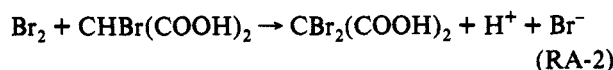
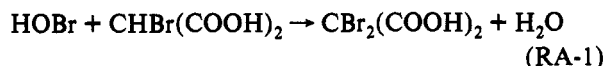
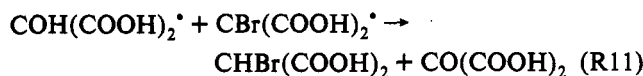
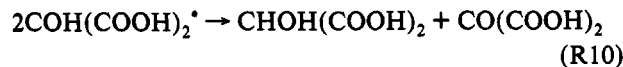
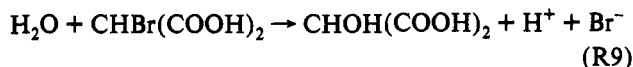
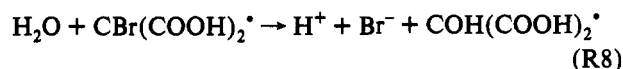
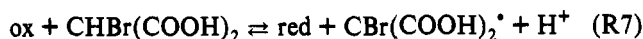
the relatively rapid decrease of  $B$ , which eventually brings the system into the oxidized state.

### Mechanism and Mathematical Model

To obtain a mathematical model, we use the Oregonator<sup>20</sup> approximation, in which the stoichiometric factor  $q$  connects the  $\text{Br}^-$  production with the oxidized catalyst consumption, instead of modeling a large set of reactions that describe the oxidative decomposition of the malonic acid bromoderivatives.

The simplified reaction scheme for the bromate-catalyst-bromomalonic acid system is as follows:





Here, "red" is the reduced form of the catalyst,  $\text{Ce}^{3+}$  or  $\text{Fe}(\text{phen})_3^{2+}$ , and "ox" is the oxidized form,  $\text{Ce}^{4+}$  or  $\text{Fe}(\text{phen})_3^{3+}$ .

We assume that reactions RA-1 and RA-2 are fast enough to neglect all other reactions of HOBr and  $\text{Br}_2$ . We consider here  $\text{CBr}_2(\text{COOH})_2$ ,  $\text{CHOH}(\text{COOH})_2$ , and  $\text{CO}(\text{COOH})_2$  as final products. We also assume that equilibrium in reaction R5c is shifted almost completely to the right.

The corresponding mathematical model is:

$$\begin{aligned} dX/dt &= -k_2h_0XY + k_3h_0XY - 2k_4^*X^2 - k_5h_0AX + k_5U^2 + k_6U(C-Z) - k_6XZ \\ dY/dt &= -k_2h_0XY - k_3h_0AY + k_8R_1 + k_9B \\ dU/dt &= 2k_5h_0AX - 2k_5U^2 - k_6U(C-Z) + k_6XZ \\ dZ/dt &= k_6U(C-Z) - k_6XZ - k_7BZ + k_7h_0R_1(C-Z) \\ dR_1/dt &= k_7BZ - k_7h_0R_1(C-Z) - k_8R_1 - k_{11}R_1R_2 \\ dR_2/dt &= k_8R_1 - 2k_{10}R_2^2 - k_{11}R_1R_2 \end{aligned} \quad (2)$$

Here,  $X = [\text{HBrO}_2]$ ,  $Y = [\text{Br}^-]$ ,  $U = [\text{HBrO}_2^*]$ ,  $Z = [\text{ox}]$ ,  $R_1 = [\text{CBr}(\text{COOH})_2^*]$ ,  $R_2 = [\text{COH}(\text{COOH})_2^*]$ ,  $A = [\text{HBrO}_3] = h_0[\text{NaBrO}_3]_0 / (0.2 + h_0)$ ,  $B = [\text{CHBr}(\text{COOH})_2]$ ,  $C = Z + [\text{red}]$ ,  $h_0 = \text{Hammett acidity function}$ ,  $k_4^* = k_4(1 + 0.87h_0)$ ,<sup>29</sup> and  $k_5$  is substituted for  $(k_{5b}k_{5c}) / (k_{5c}h_0)$ .

Assuming that the radical recombination reactions R10 and R11 are very fast, we can exclude  $R_2$  by using the quasi-steady-state approximation and obtain the following equation for  $R_1$ :

$$\frac{dR_1}{dt} = k_7BZ - k_7h_0R_1(C-Z) - \frac{k_8R_1}{q(R_1)} \quad (3)$$

where

$$\frac{1}{q(R_1)} = 1 - \frac{k_{11}^2R_1}{4k_8k_{10}} \left( 1 - \left( 1 + \frac{8k_8k_{10}}{k_{11}^2R_1} \right)^{1/2} \right)$$

If reaction R10 is much faster than reaction R11, then  $q(R_1) = 1$ ; if reaction R11 is much faster than R10, then  $q(R_1) = 0.5$ . For simplicity we use the Oregonator approach, introducing the

parameter  $q$ , which can be arbitrarily varied from 0.5 to 1, in place of  $q(R_1)$  and set  $k_8 = k_8'/q$ .

We assume also that the concentrations of bromomalonyl radical and of bromide ion are fast variables. Consequently, the reduced system of equations is:

$$\begin{aligned} \frac{dX}{dt} &= \frac{-k_2X + k_3A}{k_2X + k_3A} \left( qk_7k_8 \frac{BZ}{k_8 + k_7h_0(C-Z)} + k_9B \right) - 2k_4^*X^2 - k_5h_0AX + k_5U^2 + k_6U(C-Z) - k_6XZ \\ \frac{dU}{dt} &= 2k_5h_0AX - 2k_5U^2 - k_6U(C-Z) + k_6XZ \\ \frac{dZ}{dt} &= k_6U(C-Z) - k_6XZ - \frac{k_7k_8BZ}{k_8 + k_7h_0(C-Z)} \end{aligned} \quad (4)$$

Table I gives values of the rate constants from the literature along with those used in this paper. We used the data of Field and Försterling<sup>22</sup> as reference points to find rate constants that give a good fit of the experimental data in the temperature range 20–25 °C. To estimate changes in the rate constant values when the temperature is increased to 40 °C, we used the data of Koch and Nagy-Ungvarai<sup>30</sup> on the activation energies of reactions of oxybromine species.

We also use this model to simulate experiments in which the reductant is a mixture of malonic and bromomalonic acids. This approach is consistent with the Oregonator approximation.

To treat wave propagation, we add diffusion terms to eq 4, with  $D_x = D_u = 2 \times 10^{-5} \text{ cm}^2 \text{ s}^{-1}$  and  $D_z = 2 \times 10^{-6} \text{ cm}^2 \text{ s}^{-1}$ .<sup>31</sup>

The corresponding scaled equations are given in the Appendix.

### Simulation of the Cerium-Catalyzed System

**Shape and Amplitude of Oscillations.** Figure 2 shows  $[\text{Ce}^{4+}]$  oscillations calculated for the BZ reaction with relatively large ratio  $W$ . Their waveforms fit well those in the experiments.<sup>12,15,32</sup> This shape belongs to a generic type of simple relaxation oscillations which can be quantitatively described to first approximation by four numbers:  $M$ , the maximum concentration;  $N$ , the minimum concentration;  $T_1$ , the time of the concentration rise; and  $T_2$ , the time of the concentration fall. Table II shows good agreement between these quantities in our simulations and in experiments carried out at 40 °C.<sup>33</sup>

**Wave Speed Dependence on Bromate Concentration.** We simulated the propagation of single trigger waves in a one-dimensional excitable BZ reaction–diffusion system. As initial conditions, the variables were assigned their steady-state values for 80% of the system length. The remaining 20% of the length was filled with the estimated profile of the wave to shorten the transients and speed the occurrence of stationary propagation. The wave speed was determined during stationary propagation. Figure 3 shows the calculated wave speed dependence on  $A$  together with experimental data kindly provided by Nagy-Ungvarai.<sup>34</sup> The calculated dependence is fitted well by the following expression:

$$v(\text{mm}/\text{min}) = -3.73 + 14.75A^{0.5}$$

For the experimental data, the best fit is

$$v(\text{mm}/\text{min}) = -0.56 + 11.16A^{0.5}$$

### Simulation of the Ferriin-Catalyzed System

**Oscillations in Highly Oxidized States.** Figure 4 shows the calculated oscillations of the ferriin concentration in a system with  $W = 7.0$ . The shape of the oscillations is very close to that of the experimental curves (Figure 1).

**Propagation of Reduction Trigger Waves in the Ferriin-Catalyzed BZ System.** We simulated the propagation of catalyst

TABLE I: Rate Constants for Reactions R2–R9

catalyst	rate constant	Rovinsky and Zhabotinsky <sup>21,27</sup>	Field and Försterling <sup>22</sup>	Nagy-Ungvarai et al. <sup>11</sup>	this paper	
					40 °C	20 °C <sup>a</sup>
independent	$k_2$ (M <sup>-2</sup> s <sup>-1</sup> )	$1 \times 10^7$	$3 \times 10^6$	$1 \times 10^6$	$1.2 \times 10^7$	$7.57 \times 10^6$
	$k_{-2}$ (M <sup>-1</sup> s <sup>-1</sup> )	0	$2 \times 10^{-5}$	0	0	0
	$k_3$ (M <sup>-2</sup> s <sup>-1</sup> )	15	2	2	15	2.0
	$k_{-3}$ (M <sup>-1</sup> s <sup>-1</sup> )	0	3.2	0	0	0
	$k_4$ (M <sup>-1</sup> s <sup>-1</sup> )	$1.7 \times 10^4$	$3 \times 10^3$	$2 \times 10^3$	$1 \times 10^4$	$8.6 \times 10^3$
	$k_{-4}$ (M <sup>-1</sup> s <sup>-1</sup> )	0	$1 \times 10^{-8}$	0	0	0
	$k_5$ (M <sup>-2</sup> s <sup>-1</sup> )	100	42	40	60	10
	$k_{-5}$ (M <sup>-1</sup> s <sup>-1</sup> )	$1.2 \times 10^5$	$4.2 \times 10^7$	$4 \times 10^7$	$6 \times 10^6$	$4.2 \times 10^6$
	$k_6$ (M <sup>-1</sup> s <sup>-1</sup> )	$7.8 \times 10^3$	$8 \times 10^4$	$1 \times 10^5$	$9 \times 10^4$	$5 \times 10^4$
Ce	$k_{-6}$ (M <sup>-1</sup> s <sup>-1</sup> )	$2 \times 10^4$	$8.9 \times 10^3$	$1.1 \times 10^4$	$2.5 \times 10^4$	$2 \times 10^4$
	$k_7$ (M <sup>-1</sup> s <sup>-1</sup> )	–	–	0.4	0.8	0.4
	$k_{-7}$ (M <sup>-2</sup> s <sup>-1</sup> )	–	–	0	0	0
Fe(phen) <sub>3</sub>	$k_6$ (M <sup>-1</sup> s <sup>-1</sup> )	$1 \times 10^7$	$1 \times 10^9$	–	–	$1.66 \times 10^7$
	$k_{-6}$ (M <sup>-1</sup> s <sup>-1</sup> )	$1 \times 10^3$	33	–	–	0.3
	$k_8/k_{-7}$ (M <sup>2</sup> )	–	–	–	–	$3 \times 10^{-6}$
	$k_7 k_8/k_{-7}$ (M s <sup>-1</sup> )	$2 \times 10^{-5}$ <sup>b</sup>	–	–	–	$5 \times 10^{-7}$
independent	$k_9$ (s <sup>-1</sup> )	$1 \times 10^{-6}$	–	–	$5 \times 10^{-6}$	$3.3 \times 10^{-6}$

<sup>a</sup> This set of rate constants is used for simulations of experiments carried out at  $T = 20$  °C<sup>22</sup> and 25 °C in this paper and in refs 9, 11, and 12. <sup>b</sup> This value is for  $k_7 k_8/k_{-7}$ .

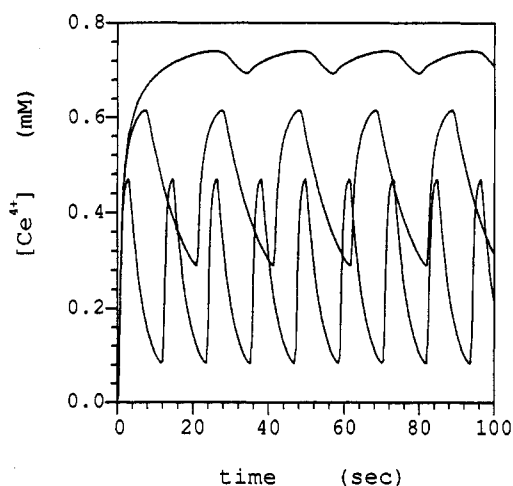


Figure 2. Calculated oscillations of  $[Ce^{4+}]$ . Initial reagent concentrations (M):  $A = 0.1$ ;  $h_0 = 4.0$ ;  $C = 1.0 \times 10^{-3}$ ;  $B$  (from top to bottom) = 0.032, 0.1, 0.32;  $q = 0.6$ ;  $T = 40$  °C.

reduction trigger waves in a one-dimensional excitable system to model the experiments by Smoes.<sup>9</sup> Initial conditions were set as follows: variables were assigned their steady-state values for 90% of the system length; in the remaining 10%, the initial concentration of  $HBrO_2$  was reduced to 0.2 of its steady-state value with the other variables remaining at their steady-state values. The perturbation excited the neighboring points and induced the trigger wave front of catalyst reduction. Later, a reverse wave front of catalyst oxidation appeared and propagated with a higher speed. The speed of this wave back decreased when it approached the leading wave front. Figure 5a ( $W = 1.25$ ) shows stationary wave propagation that occurs after a transition period. Figure 5b shows that decremental propagation takes place at a higher  $h_0 A/B$  ratio ( $W = 1.325$ ).

Figure 6 shows trajectories of the fronts and backs of the waves shown in Figure 5. The solid line corresponds to decremental trigger wave propagation and the dashed line to stationary propagation.

## Discussion

Studies of generic models<sup>7,8</sup> demonstrate that the stability of stationary propagation of periodic waves in reaction–diffusion systems decreases when the length of the “excited” part of the wave becomes significant in comparison with the wavelength. As a result, new types of spatio-temporal structures appear. Some apparently related phenomena have been observed in experiments in the BZ reaction–diffusion system.<sup>3–6</sup>

Here we have presented a mathematical model of the BZ reaction that gives for the first time a good semiquantitative simulation of oscillations and waves when the period of catalyst oxidation is not short in comparison with the period of catalyst reduction. The model, which is of the Oregonator class, is valid for both cerium and ferroin catalyzed systems. Such simplified models are necessary for simulation of chemical wave propagation and other spatio-temporal phenomena in reaction–diffusion systems because of the prohibitive size of calculations that employ more detailed descriptions. We hope that our model will make possible the analysis and quantitative description of such phenomena in the BZ system.

We have performed simulations of experiments carried out in a wide range of initial reagent concentrations. We first checked whether the model is able to simulate correctly the shape of oscillations in well-stirred reactors. Oscillations in the cerium-catalyzed BZ reaction were quantitatively studied in refs 32 and 33 in wide ranges of concentrations of bromate and bromomalonic acid with  $[H_2SO_4] = 1.5$  M at 40 °C. The simulated wave forms shown in Figure 2 are very close to the experimental ones. Table II gives a quantitative comparison of the calculated and experimental data. The agreement is good, though in two experiments the calculated minimum concentrations of  $Ce^{4+}$  are significantly less than the experimental values, and the calculated  $T_2$  values are correspondingly larger. Comparison of Figures 1 and 4 shows that the model successfully simulates oscillations in the ferroin-catalyzed BZ reaction when the catalyst is almost totally oxidized during about half the period of oscillation.

The calculated wave velocity increases as the square root of the bromate concentration in the Ce-catalyzed system, in agreement with the experimental data of Nagy-Ungvarai<sup>34</sup> (Figure 3). Our model simulates a transient process of compression of the catalyst reduction wave experimentally observed by Smoes<sup>9</sup> (Figure 6). The wave compression results in either establishment of a stationary wave (Figure 5a) or annihilation of the wave (Figure 5b).

Initially we used the rate constants given by Field and Försterling.<sup>22</sup> However, we were unable to obtain the experimentally observed dependence of the Ce wave speed on the bromate concentration with these parameters. To obtain this dependence, we decreased  $k_{-3}$  by a factor of 10. The main purpose of this change was to increase the role of reaction R6 relative to R5 in controlling the equilibrium between  $[HBrO_2]$  and  $[HBrO_2^*]$ . We also changed  $k_2$ ,  $k_4$ ,  $k_5$ , and  $k_{-6}$  several-fold in order to achieve a better fit of the experimental data. With this set of rate constants (Table I), we were able to simulate all the experiments in the 20–25 °C range.

**TABLE II: Characteristic Values of Experimental<sup>33</sup> and Calculated Oscillations in the Ce-BMA System<sup>a</sup>**

<i>A</i> (M)	<i>B</i> (M)	<i>M</i> <sub>ex</sub> (% C)	<i>M</i> <sub>cal</sub> (% C)	<i>N</i> <sub>ex</sub> (% C)	<i>N</i> <sub>cal</sub> (% C)	<i>T</i> <sub>1ex</sub> (s)	<i>T</i> <sub>1cal</sub> (s)	<i>T</i> <sub>2ex</sub> (s)	<i>T</i> <sub>2cal</sub> (s)
0.05	0.01	78	76	72	68	30	59	23	28
0.05	0.032	65	63	47	28	13	20	20	51
0.05	0.1	52	50	26	6.8	6.0	7.0	17	31
0.1	0.032	75	74	68	69	13	14	9.0	8.6
0.1	0.1	64	62	44	29	5.0	6.8	9.0	13.5
0.1	0.32	40	47	17	8.4	2.0	2.8	7.0	8.9

<sup>a</sup> Designations: *M*<sub>ex</sub>, *M*<sub>cal</sub>: experimental and calculated maximum values of [Ce<sup>4+</sup>] in oscillatory cycle. *N*<sub>ex</sub>, *N*<sub>cal</sub>: minimum values of [Ce<sup>4+</sup>] in oscillatory cycle. *T*<sub>1</sub>: duration of [Ce<sup>4+</sup>] increase. *T*<sub>2</sub>: duration of [Ce<sup>4+</sup>] decrease. Other parameters: *C* = 0.001 M, *h*<sub>0</sub> = 4.0. Simulations were made with *q* = 0.6.

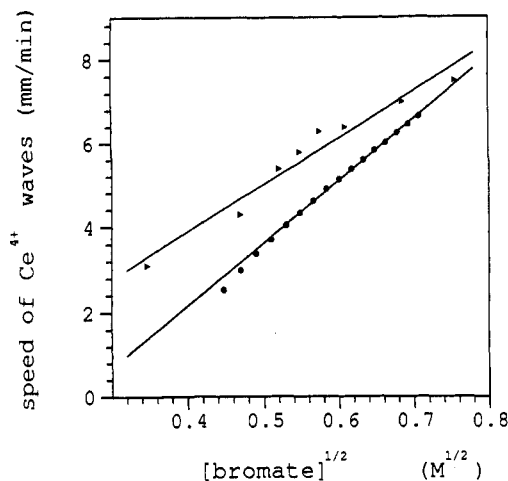


**Figure 3.** Dependence of trigger wave speed on bromate concentration (*A*) in the cerium-catalyzed BZ reaction-diffusion system. Circles—simulation, parameters: *h*<sub>0</sub> = 0.6, *C* = 3 × 10<sup>-3</sup> M, *B* = 0.12 M, *q* = 0.9 (*T* = 25 °C). Solid line, fitting of the calculated points:  $v = -3.73 + 14.75A^{0.5}$ . Triangles—experimental data,<sup>34</sup> parameters: *h*<sub>0</sub> = 0.6, *C* = 3 × 10<sup>-3</sup> M, *B* = 0.12 M, *T* = 25 °C. Solid line, fitting of the experimental points:  $v = -0.56 + 11.16A^{0.5}$ .

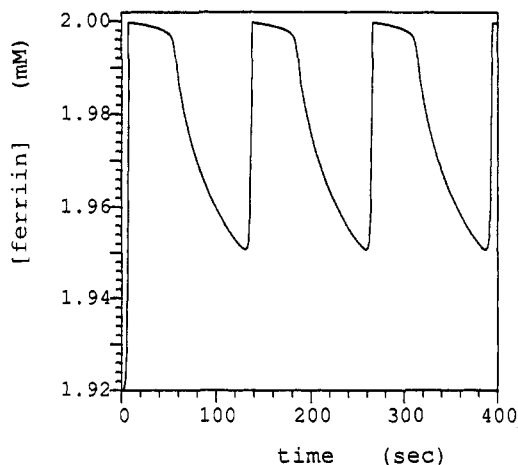


**Figure 4.** Calculated oscillations in ferriin concentration. Parameters (M): *A* = 0.25, *h*<sub>0</sub> = 0.59, *C* = 2 × 10<sup>-3</sup>, *B* = 0.016, *q* = 0.5, *T* = 20 °C.

Our model differs from previous models of this type<sup>11,21,35</sup> by its explicit inclusion of [BrO<sub>2</sub><sup>\*</sup>]. One may ask whether such an extension of the model is necessary. The scaling of the Ce-related version given in the Appendix shows that the ratio of the time scale for [HBrO<sub>2</sub><sup>+</sup>] (*u*) to that of [HBrO<sub>2</sub>] (*x*) is *k*<sub>-6</sub>/*k*<sub>6</sub>. This ratio is about 0.1 with rate constants from refs 11 and 22. In this case, *u* is a fast variable with respect to *x*, and it can be dropped from the model, as was done in ref 11. However, this set of rate constants does not fit well the experimental dependence of the wave speed on bromate concentration. We find that *k*<sub>-6</sub>/*k*<sub>6</sub> = 0.4. With this rate constant ratio, reduction of the model to the two-variable (*x*, *z*) version will result in significant discrepancies. For the ferriin-catalyzed reaction, the scaling given in the

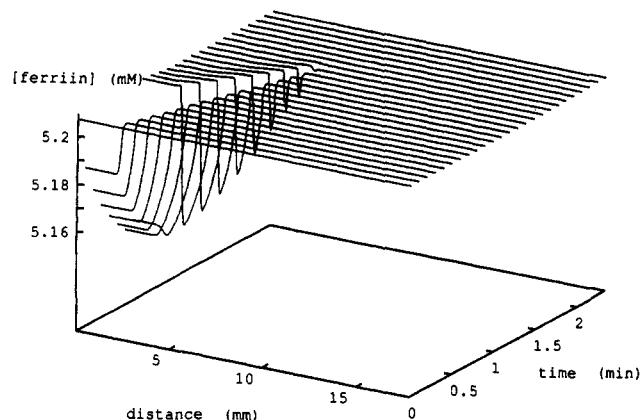
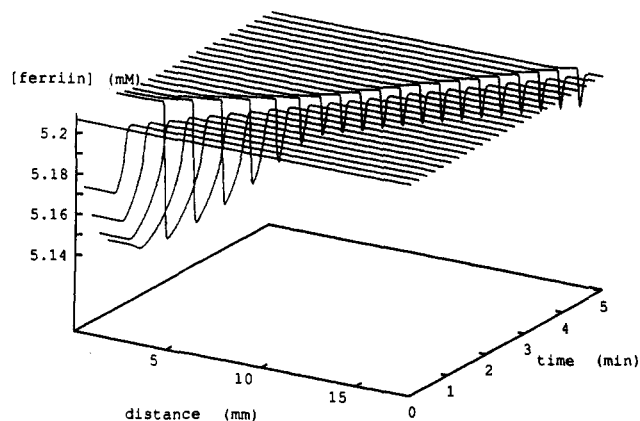


**Figure 5.** Calculated trigger wave propagation in the ferriin-catalyzed BZ reaction-diffusion system. Parameters (M): *A* = 0.4, *C* = 5.21 × 10<sup>-3</sup>, *B* = 0.16, *q* = 0.5, *T* = 20 °C. (a, top) *h*<sub>0</sub> = 0.5, stationary propagation. (b, bottom) *h*<sub>0</sub> = 0.53, decremental propagation.

Appendix shows that reduction to the *x*,*z*-model can be made without significant error.

Many workers have employed aqueous solutions of malonic acid brominated according to eq 1 for studying chemical waves<sup>1,11,26</sup> in the belief that this preparation contains mainly bromomalonic acid. Recently, Försterling et al.<sup>25</sup> showed that at high acidity the rate of bromomalonic acid bromination is 2.5-fold larger than that of malonic acid. As a result, bromination proceeds according to eq 1 only until about 10% of malonic acid is brominated. After that, a significant bromination of bromomalonic acid begins. If the total initial amount of Br is equal to that of malonic acid, the final solution will contain approximately 40% of malonic acid, 40% of a mixture of dibromomalonic and dibromoacetic acids, and only about 20% of bromomalonic acid.<sup>25</sup>

Still, this preparation remains a convenient tool for experimental study of new oscillating and wave modes in the BZ reaction when relatively high initial concentrations of bromomalonic acid are needed. We compared it with mixtures of CH<sub>2</sub>(COOH)<sub>2</sub> and CHBr(COOK)<sub>2</sub>. Almost identical oscillations (Figure 1b) were observed with either this preparation at a concentration of 0.03 M or the corresponding mixture of malonic (0.012 M) and

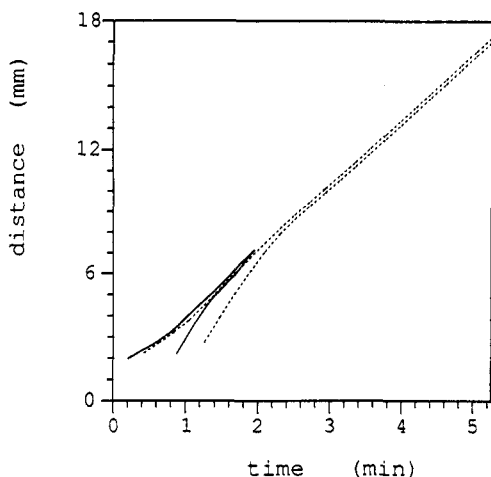


Figure 6. Trajectories of the wave front and the wave back for stationary and decremental trigger wave propagation shown in Figure 5. Solid line, decremental propagation; dashed line, stationary propagation.

bromomalonic (0.006 M) acids, in good agreement with the results of ref 25 on the composition of this preparation.

We used data by Rovinsky<sup>36</sup> on the kinetics of reduction of ferriin by bromomalonic acid<sup>26</sup> to estimate the rate constants for simulating experiments on ferriin-catalyzed oscillations and on waves in systems containing either the preparation of ref 26 or malonic acid in low concentrations.

Our scheme, R7–R11, permits the stoichiometric coefficient  $q$  to be varied from 0.5 to 1.0, and we used  $q$  as another fitting parameter. Försterling et al.<sup>25</sup> showed that during reduction of  $Ce^{4+}$  by bromomalonic acid  $q = 0.5$  when the system is deoxygenated and  $q = 1$  when the solution contains  $O_2$ . These data imply, in the scope of scheme R7–R11, that reaction R11 is much faster than reaction R10 in an oxygen-free solution. If  $O_2$  reacts with bromomalonyl radical to prevent reaction R11, without interfering with the hydrolysis of the radical, we will have  $q = 1$ . Note that our reactions R8, R10, and R11 are equivalent to reactions R4 and R5 in ref 25 with respect to the initial and final species.

Many variants and extensions of our scheme R1–RA-2 can be written for the BZ reaction with both malonic and bromomalonic acids as the initial reagents. However, there is insufficient experimental work on the organic aspects of the system to justify detailed modeling at the present time. On the other hand, this work, along with many earlier studies, shows that the Oregonator approximation can give accurate modeling if one replaces this complex reaction network by a simple stoichiometric relation between  $Br^-$  production and catalyst reduction.

For the ferriin-catalyzed reaction, some other problems remain. In our experiments, a slow decrease of the total concentration of the ferriin catalyst was observed. This effect may result from formation of a ferriin–bromine adduct as proposed by Kéki et al.<sup>37</sup> Further experiments are required to check this hypothesis and to elucidate the reaction mechanism. Inclusion of the two-electron oxidation of ferriin by bromine species<sup>37,38</sup> may improve significantly the simulation of experimental data in the ferriin-catalyzed BZ system.

In this paper, we use a batch model along with the stationary approximation for concentrations of the initial reagents. Such a model is valid only for simulation of the system during the first few oscillatory cycles. Extended models are required to simulate the long-time behavior of the system. In our CSTR experiments, we used a residence time much larger than the oscillation period. Nevertheless, flow terms should be included in the model for quantitative simulation of the CSTR experiments.

**Acknowledgment.** This work was supported by NSF Grant CHE-9023294. We thank Z. Nagy-Ungvarai for providing her

unpublished experimental results, M. Eager for supplying dipotassium bromomalonate, and K. Kustin and L. Györgyi for helpful discussions.

## Appendix

**Scaling of the Model.** 1. For the cerium-catalyzed reaction, a scaling, appropriate for intermediate values of  $z$ , gives the following equation:

$$\epsilon_1 x_\tau = -\eta x^2 - \gamma x + \delta u^2 + u(1-z) - xz + (qz + \beta) \frac{\mu - x}{\mu + x} + \epsilon_1 dx_{\xi\xi}$$

$$\epsilon_2 u_\tau = 2\gamma x - 2\delta u^2 - u(1-z) + xz + \epsilon_2 du_{\xi\xi}$$

$$z_\tau = u(1-z) - xz - z + z_{\xi\xi} \quad (A1)$$

where

$$X = \frac{k_7 B}{k_6} x, \quad U = \frac{k_7 B}{k_6} u, \quad Z = Cz, \quad t = \frac{\tau}{k_7 B}, \quad r = \left( \frac{D_z}{k_7 B^2} \right)^{1/2},$$

$$\epsilon_1 = \frac{k_7 B}{k_6 C}, \quad \epsilon_2 = \frac{k_7 B}{k_6 C}, \quad \beta = \frac{k_9}{k_7 C}, \quad \mu = \frac{k_3 k_6 A}{k_2 k_7 B}, \quad \eta = \frac{2k_4 k_7 B}{k_6^2 C},$$

$$\gamma = \frac{k_5 h_0 A}{k_6 C}, \quad \delta = \frac{k_5 k_7 B}{k_6^2 C}, \quad d = \frac{D_x}{D_z} = \frac{D_u}{D_z}$$

2. The above scaling is not valid for the ferriin-catalyzed reaction because  $k_6$  is very small in this system. We instead use the following scaled equations:

$$\epsilon_1 x_\tau = -x^2 - x + \epsilon_2 \gamma u^2 + u(1-z) - \delta xz + \left( q\alpha \frac{z}{\epsilon_3 + 1 - z} + \beta \right) \frac{\mu - x}{\mu + x} + \epsilon_1 dx_{\xi\xi}$$

$$\epsilon_2 u_\tau = 2x - 2\epsilon_2 \gamma u^2 - u(1-z) + \delta xz + \epsilon_2 du_{\xi\xi}$$

$$z_\tau = u(1-z) - \delta xz - \alpha \frac{z}{\epsilon_3 + 1 - z} + z_{\xi\xi} \quad (A2)$$

where

$$X = \frac{k_5 h_0 A}{2k_4^*} x, \quad U = \frac{(k_5 h_0 A)^2}{2k_4^* k_6 C} u, \quad Z = Cz,$$

$$t = \frac{2k_4^* C}{(k_5 h_0 A)^2} \tau = T_* \tau, \quad r = (T_* D_z)^{1/2} \xi,$$

$$\epsilon_1 = \frac{k_5 h_0 A}{2k_4^* C}, \quad \epsilon_2 = \frac{(k_5 h_0 A)^2}{2k_4^* k_6 C^2}, \quad \epsilon_3 = \frac{k_8}{k_7 h_0 C}$$

$$\alpha = \frac{2k_4^* k_7 k_8 B}{k_5^2 k_7 h_0^3 A^2}, \quad \beta = \frac{2k_4^* k_9 B}{(k_5 h_0 A)^2},$$

$$\mu = \frac{2k_3 k_4^*}{k_2 k_5 h_0}, \quad \gamma = \frac{k_5}{k_6}, \quad \delta = \frac{k_6 C}{k_5 h_0 A}, \quad d = \frac{D_x}{D_z} = \frac{D_u}{D_z},$$

$$X = [HBrO_2], \quad U = [HBrO_2^+], \quad Z = [Fe(phen)_3^{3+}],$$

$$A = [HBrO_3], \quad B = [CHBr(COOH)_2],$$

$$C = [Fe(phen)_3^{3+}] + [Fe(phen)_3^{2+}],$$

$$h_0 = \text{Hammet acidity function},$$

$$D_i = \text{diffusion coefficients}$$

Replacing  $z$  by

$$a = \frac{1}{\epsilon_3 + 1 - z} \quad (\text{A3})$$

yields the following system:

$$\epsilon_1 x_\tau = -x^2 - x + \epsilon_2 \gamma u^2 + u \left( \frac{1}{a} - \epsilon_3 \right) - \delta x \left( 1 + \epsilon_3 - \frac{1}{a} \right) + (q\alpha(a + a\epsilon_3 - 1) + \beta) \frac{\mu - x}{\mu + x} + \epsilon_1 dx_{\xi\xi}$$

$$\epsilon_2 u_\tau = 2x - 2\epsilon_2 \gamma u^2 - u \left( \frac{1}{a} - \epsilon_3 \right) + \delta x \left( 1 + \epsilon_3 - \frac{1}{a} \right) + \epsilon_2 du_{\xi\xi}$$

$$a_\tau = a[u(1 - a\epsilon_3) - \delta x(a + a\epsilon_3 - 1) - \alpha a(a + a\epsilon_3 - 1)] + a_{\xi\xi} - \frac{2(a_\xi)^2}{a} \quad (\text{A4})$$

## References and Notes

- (1) Field, R. J., Burger, M., Eds. *Oscillations and Traveling Waves in Chemical Systems*; Wiley: New York, 1985.
- (2) Swinney, H. L., Krinsky, V. I., Eds. *Waves and Patterns in Chemical and Biological Media*. *Physica D* **1991**, *49* (1 & 2).
- (3) Vidal, C.; Pagola, A.; Bodet, J. M.; Hanusse, P.; Bastardie, E. *J. Phys.* **1986**, *47*, 1999.
- (4) Maselko, J.; Reckley, J. S.; Showalter, K. *J. Phys. Chem.* **1989**, *93*, 2774.
- (5) Zhabotinsky, A. M. In *Oscillating Processes in Biological and Chemical Systems*; Frank, G. M., Ed.; Nauka: Moscow, 1967; p 252.
- (6) Zhabotinsky, A. M. In *Biological and Biochemical Oscillators*; Chance, B., Ed.; Academic Press: New York, 1973; p 89.
- (7) Krinsky, V. I. *Prob. Cybernet.* **1968**, 20.
- (8) Zykov, V. S. *Simulation of Wave Processes in Excitable Media*; Manchester University Press: Manchester, England, 1988.
- (9) Smoes, M.-L. In *Dynamics of Synergetic Systems*; Haken, H., Ed.; Springer: Berlin, 1980; p 80.
- (10) Tyson, J. J.; Fife, P. C. *J. Chem. Phys.* **1980**, *73*, 2224.
- (11) Nagy-Ungvarai, Z.; Tyson, J. J.; Hess, B. *J. Phys. Chem.* **1989**, *93*, 707.
- (12) Nagy-Ungvarai, Z.; Müller, S. C.; Tyson, J. J.; Hess, B. *J. Phys. Chem.* **1989**, *93*, 2760.
- (13) Belousov, B. P. In *Coll. Ref. Rad. Med. 1958*; Med-Press: Moscow, 1959; p 145.
- (14) Zhabotinsky, A. M. *Biofizika* **1964**, *9*, 306.
- (15) Zhabotinsky, A. M. *Proc. Acad. Sci. USSR* **1964**, *157*, 392.
- (16) Vavilin, V. A.; Zhabotinsky, A. M. *Kinet. Katal.* **1969**, *10*, 83.
- (17) Vavilin, V. A.; Zhabotinsky, A. M. *Kinet. Katal.* **1969**, *10*, 657.
- (18) Vavilin, V. A.; Zhabotinsky, A. M.; Zaikin, A. N. In *Biological and Biochemical Oscillators*; Chance, B., Ed.; Academic Press: New York, 1973; p 71.
- (19) Field, R. J.; Körös, E.; Noyes, R. M. *J. Am. Chem. Soc.* **1972**, *94*, 8649.
- (20) Field, R. J.; Noyes, R. M. *J. Chem. Phys.* **1974**, *60*, 1877.
- (21) Rovinsky, A. B.; Zhabotinsky, A. M. *J. Phys. Chem.* **1984**, *88*, 6081.
- (22) Field, R. J.; Försterling, H.-D. *J. Phys. Chem.* **1986**, *90*, 5400.
- (23) Försterling, H.-D.; Muranyi, S.; Noszticzius, Z. *J. Phys. Chem.* **1990**, *94*, 2915.
- (24) Robertson, E. B.; Dunford, H. B. *J. Am. Chem. Soc.* **1964**, *86*, 5080.
- (25) Försterling, H.-D.; Stuk, L.; Barr, A.; McCormick, W. D. *J. Phys. Chem.* **1993**, *97*, 2623.
- (26) Zaikin, A. N.; Zhabotinsky, A. M. *Nature* **1970**, *225*, 535.
- (27) Press, W. H.; Flannery, B. P.; Teukolsky, S. A.; Vetterling, W. T. *Numerical Recipes (FORTRAN Version)*; Cambridge University Press: Cambridge, 1989.
- (28) Zhabotinsky, A. M.; Rovinsky, A. B. *J. Phys. Chem.* **1990**, *94*, 8001.
- (29) Knight, G. C.; Thompson, R. C. *Inorg. Chem.* **1973**, *12*, 63.
- (30) Koch, E.; Nagy-Ungvarai, Z. *Ber. Bunsen-Ges. Phys. Chem.* **1987**, *91*, 1375.
- (31) Ruff, I.; Zimonyi, M. *Magyar Kem. Foly.* **1973**, *79*, 135.
- (32) Vavilin, V. A.; Zhabotinsky, A. M.; Krupyanko, V. I. In *Oscillating Processes in Biological and Chemical Systems*; Frank, G. M., Ed.; Nauka: Moscow, 1967; p 199.
- (33) Zhabotinsky, A. M.; Zaikin, A. N.; Korzukhin, M. D.; Kreitzer, G. *P. Kinet. Katal.* **1971**, *12*, 584.
- (34) Nagy-Ungvarai, Z., personal communication.
- (35) Tyson, J. J. *Ann. N.Y. Acad. Sci.* **1979**, *316*, 279.
- (36) Rovinsky, A. B. *J. Phys. Chem.* **1984**, *88*, 4.
- (37) Kéki, S.; Magyar, I.; Beck, M. T.; Gáspár, V. *J. Phys. Chem.* **1992**, *96*, 1725.
- (38) Noyes, R. M. *J. Am. Chem. Soc.* **1980**, *102*, 4644.